# Functional trade-offs are driven by coordinated changes among cell types in the wood of angiosperm trees from different climates

Guangqi Zhang, Zhun Mao, Pascale Maillard, Loïc Brancheriau, Bastien Gérard, Julien Engel, Claire Fortunel, Patrick Heuret, Jean-luc Maeght, Jordi Martínez-Vilalta, et al.

Full paper

New Phytologist

# Functional trade-offs are driven by coordinated changes among cell types in the wood of angiosperm trees from different climates

**Guangqi Zhang[1,2], Zhun Mao[1], Pascale Maillard[2], Loïc Brancheriau[3,4], Bastien Gérard[2], Julien Engel[1], Claire Fortunel[1], Patrick Heuret[1], Jean-Luc Maeght[1], Jordi Martínez-Vilalta[5,6] and Alexia Stokes[1]**

[1]AMAP, University of Montpellier, CIRAD, CNRS, INRAE, IRD, Montpellier, 34000, France; [2]SILVA, INRAE, Université de Lorraine, Agroparistech, Centre de Recherche Grand-Est Nancy, Champenoux, 54280, France; [3]CIRAD, UPR BioWooEB, Montpellier, 34000, France; [4]BioWooEB, University of Montpellier, CIRAD, Montpellier, 34000, France; [5]CREAF, Bellaterra (Cerdanyola del Vallès), Catalonia, E08193, Spain; [6]Universitat Autònoma Barcelona, Bellaterra (Cerdanyola del Vallès), Catalonia, E08193, Spain

Author for correspondence:
*Guangqi Zhang*
*Email*: zh.guangqi@gmail.com

Received: *6 March 2023*
Accepted: *20 June 2023*

*New Phytologist* (2023) **240:** 1162–1176
**doi**: 10.1111/nph.19132

**Key words:** anatomical traits, biome, fibre, parenchyma, vessel, xylem density.

## Summary

- Wood performs several functions to ensure tree survival and carbon allocation to a finite stem volume leads to trade-offs among cell types. It is not known to what extent these trade-offs modify functional trade-offs and if they are consistent across climates and evolutionary lineages.
- Twelve wood traits were measured in stems and coarse roots across 60 adult angiosperm tree species from temperate, Mediterranean and tropical climates.
- Regardless of climate, clear trade-offs occurred among cellular fractions, but did not translate into specific functional trade-offs. Wood density was negatively related to hydraulic conductivity ($K_{th}$) in stems and roots, but was not linked to nonstructural carbohydrates (NSC), implying a functional trade-off between mechanical integrity and transport but not with storage. NSC storage capacity was positively associated with $K_{th}$ in stems and negatively in roots, reflecting a potential role for NSC in the maintenance of hydraulic integrity in stems but not in roots. Results of phylogenetic analyses suggest that evolutionary histories cannot explain covariations among traits.
- Trade-offs occur among cellular fractions, without necessarily modifying trade-offs in function. However, functional trade-offs are driven by coordinated changes among xylem cell types depending on the dominant role of each cell type in stems and roots.

## Introduction

Tree wood is multifunctional, simultaneously providing hydraulic transport, mechanical integrity, storage and defence against pest/pathogen attack (Chave *et al.*, 2009). The secondary wood of angiosperms comprises three main cell types (parenchyma, vessels and fibres) that contribute to these distinct functions. The metabolically active radial and axial parenchyma (RAP) cells play a fundamental role in defence and wound repair (Morris *et al.*, 2020), respiration (Rodríguez-Calcerrada *et al.*, 2015), carbohydrate, nutrient and water storage (Plavcová *et al.*, 2016; Secchi *et al.*, 2017); vessels mainly provide long-distance water and nutrient transport (Tyree & Ewers, 1991; Pratt & Jacobsen, 2017); and fibres, as well as lignified parenchyma, provide mechanical strength (Burgert & Eckstein, 2001; Rana *et al.*, 2009; Ziemińska *et al.*, 2013; Fortunel *et al.*, 2014). Trees have evolved in response to a multitude of diverse environmental factors that have led to trade-offs in functions within the xylem space (Baas *et al.*, 2004; Lachenbruch & McCulloh, 2014; Grubb, 2016; Pratt & Jacobsen, 2017; Pratt *et al.*, 2021a). The resulting structure of the xylem space actively influences physiological processes occurring within trees, potentially driving survival or failure when local environmental conditions change (Jacobsen *et al.*, 2007; Choat *et al.*, 2018).

Wood cellular composition is widely divergent among woody angiosperms. Due to the finite volume or given cross-sectional area, Pratt and Jacobsen (2017) described that proportional trade-offs occurred among the major cell types, with strong and negative correlations between fibre and RAP fractions and between fibre and vessel fractions (VFs). However, Fortunel *et al.* (2014) found a negative relationship between fibre and parenchyma fractions, but no relationship with VFs across 113 Amazonian rainforest tree species and Pratt and Jacobsen (2017) also found that vessel and parenchyma fractions were not correlated with each other across 36 shrub species. This divergence in wood cell fractions raises important questions regarding trade-offs between functions. Whether the allocation trade-off among cellular types really reflects the trade-off in function is not clear, as cell types and functions are entwined and connected in complex ways.

As the largest metabolically active wood fraction, parenchyma cells and the nonstructural carbohydrates (NSC) stored within them play key roles, for example, for resprouting after disturbance (Smith *et al.*, 2018). Axial parenchyma (AP) is also associated with the maintenance of hydraulic conductivity, as angiosperm tree species with higher fractions of AP tend to have larger vessels (Morris *et al.*, 2018), greater hydraulic capacitance (Ziemińska *et al.*, 2020; Aritsara *et al.*, 2021) and lower vulnerability to xylem embolism (Kiorapostolou *et al.*, 2019). Radial parenchyma (RP) is not only a major NSC storage compartment but can also contain a large amount of lignin between individual parenchyma cells and surrounding fibres, thus potentially increasing overall wood density (WD) and improving radial strength (Burgert & Eckstein, 2001; Zhang *et al.*, 2022b), but decreasing the available wood space for other cell types. The presence of large or abundant vessels can result in decreased WD, but a large lumen fraction may be important for increased hydraulic conductivity (Zanne *et al.*, 2010), potentially creating a trade-off between hydraulics and xylem mechanical integrity (Christensen-Dalsgaard *et al.*, 2007a,b; Chen *et al.*, 2020), although studies provide conflicting results. For example, Woodrum *et al.* (2003) found no relationship between hydraulic conductivity and xylem modulus of elasticity (i.e. resistance to being deformed elastically) in several diffuse-porous *Acer* species. Differences in function among species may be due to the spatial organization of cell types, but the link between wood function and its spatial structure is still poorly understood. Although there have been several studies on the trade-offs in functions performed by different cell types (Supporting Information Table S1), few have done so across a broad range of tree species from different climates.

Testing hypotheses about the links between wood structures and functions can be facilitated by studying patterns within trees, and in particular, comparing stem and root wood. Regardless of the porosity type in angiosperm stems (i.e. ring- or diffuse-porous), wood becomes more diffuse-porous with distance from the stem in coarse roots (Patel, 1965). Roots usually have fewer vessels and smaller fibre fraction, but greater RAP fraction than stems (see Stokes & Guitard, 1997), thus increasing NSC storage capacity. This gradient in porosity in roots is advantageous for an improved hydraulic efficiency, especially in horizontal lateral roots that take up water from the most superficial soil layers (Fahn, 1967; Pratt *et al.*, 2007). Also, when responding to mechanical stress, such as wind loading, root system anchorage is better improved through morphological changes, rather than modifications in xylem anatomy (Stokes & Guitard, 1997).

Due to the different plant strategies of temperate, Mediterranean and tropical climates as well as wet vs dry conditions, there is likely to be a divergence in wood structure. Tropical trees typically possess wider vessels and more parenchyma than temperate tree species (McCulloh *et al.*, 2010; Morris *et al.*, 2016, 2018), resulting in different wood densities. Despite the numerous studies focussing on variation and functional significance of xylem properties, it remains unclear how patterns of xylem traits and function are altered across different climates and whether functional trade-offs vary due to climate differences.

Allocation to different wood cell types and resulting functional strategies may be driven by coordinated evolutionary constraints. Exploring phylogenetically independent relationships among wood functional traits should provide us with a more genuine insight for correlated evolutionary shifts and their impact on trait variation (Felsenstein, 1985). For example, phylogeny explained more than half of the variation in *individual* functional traits in the stem xylem of 700 angiosperm tree species in China (Zheng *et al.*, 2019). However, when examining the relationships among traits (e.g. WD and fibre fraction, hydraulic conductivity and embolism resistance, or NSC content and parenchyma fractions), studies have shown that these relationships are not necessarily affected by evolutionary history (Fortunel *et al.*, 2014; Levionnois *et al.*, 2021; Pratt *et al.*, 2021b; Zhang *et al.*, 2022b). Nonetheless, in order to identify trade-offs between anatomical structure and xylem function, phylogenetic analysis is still needed, especially across a broad range of species and climates.

We investigated the covariation in 12 wood traits in stems and coarse roots of 60 angiosperm tree species from temperate, Mediterranean and tropical climates. We asked whether the design of the xylem space captures trade-offs among the three main wood functions in stems and roots and whether this coordination is linked to climate or constrained by evolutionary histories. We hypothesize that (H1) coarse root wood will have more parenchyma and NSC, but lower WD than stem wood and that this pattern will be more pronounced in tropical species. (H2) Due to spatial constraints in a finite stem volume, we expect an allocation-driven trade-off among parenchyma, fibre and VFs. (H3) Due to the multiplicity of traits involved in a given function, functional trade-offs will be less clear than allocation-driven trade-offs between cell type fractions and will also differ between stems and coarse roots, as the relative importance change (e.g. the mechanical integrity of xylem tissue is less important in roots than stems). (H4) Due to the divergence of wood traits across climates, we expect that relationships among functions will also differ. For example, as the seasonal dormancy of temperate and Mediterranean species is more pronounced than that of trees in the tropics, we suppose that high levels of NSC are needed to assure the production of new and large earlywood vessels, especially in ring-porous species.

## Materials and Methods

### Study sites, species and sampling

This study was conducted on trees from forests growing in three different climates: a temperate forest (Luz-Saint-Sauveur, France; 42°52′25″N, 0°0′26″E), a Mediterranean forest (Montpellier, France; 43°38′46″N, 4°0′3″E) and a tropical forest (Paracou, French Guiana; 5°16′32″N, 52°55′28″W). The Luz-Saint-Sauveur site has a temperate mountain climate, with the heavy rainfall in first half of a year. The mean annual precipitation is 1217 mm, and the mean annual temperature is 11.8°C. The Montpellier site has a typical Mediterranean climate with hot dry summers and cool wet winters. The mean annual precipitation is 588 mm with *c.* 80% of the annual rainfall occurring between

September and April. The mean annual temperature is 15.4°C. The Paracou site has a typical tropical rainforest climate with a distinct dry season from mid-August to mid-November and long rainy season often interrupted by a short drier period between March and April. The mean annual precipitation is 3035 mm with a minimum in September and maximum in May. The mean annual temperature is 26.9°C. The temperature and precipitation data were calculated using mean monthly data from the past 31 yr (Fig. S1: data are from Meteo-France; https://meteofrance.com/).

A total of 60 angiosperm species were selected, with 20 species in each climate, spanning 43 genera and 32 families (Table S2; Zhang *et al.*, 2022a). The selected tree species are commonly found in these forests and represent their dominance to a certain extent. For each species, three healthy, adult, single-stemmed trees were identified, with a distance of at least 20 m between them. Selected stems were between 0.1 and 0.5 m wide at a height of 1.3 m (however, in some adult, small-stature species, diameter was as small as 0.05 m; Table S2). For Mediterranean and tropical trees, samples were collected at the end of August and September 2019, and for temperate trees, samples were collected in September 2020. Although phenological stages differ between tree species, we assumed that NSC would be greatest in temperate and Mediterranean species at the end of the summer season, but that little difference occurs in tropical species throughout the year (Martínez-Vilalta *et al.*, 2016). We sampled all trees between 7:00 h and midday, to reduce variability in NSC content linked to photosynthate production. At a height of 1.3 m, three 0.05-m-long cores were extracted from tree stems with a 4.3-mm-diameter increment borer ($n = 540$). To collect samples of roots, we excavated a single lateral root (0.02–0.05 m in diameter) and at a distance of 0.3–0.5 m from the base of the tree, we extracted three increment cores or sampled three 0.02-m-long segments of root, depending on accessibility ($n = 540$). All samples were immediately placed in moist paper, put in a cooler box and taken to the laboratory before midday, where they were kept in a fridge at 4°C.

## Measurement of wood traits

**Xylem anatomical traits** Within 24 h, one of the three replicate increment cores was trimmed and a 0.02-m-long section was taken from the outer sapwood and placed in a 50% solution of alcohol and water. A 0.02-m-long section of root was also placed in the solution of alcohol and water. These sections were kept for the analysis of anatomical traits. Increment cores were embedded in paraffin individually after dehydration by immersing in a sequence of alcohol solution, whereas sections of root were clamped in a microtome. We used a sliding microtome to cut 15- to 20-µm-thick cross-sections. Cross-sections were stained with a mixture of safranin and Alcian blue (0.35 g safranin in 35 ml 50% alcohol with 0.65 g Alcian blue in 65 ml deionized water) and dehydrated using ethanol series (50%, 75%, 95% and 100%). Finally, sections were mounted on glass slides and observed under a light microscope (Olympus BX 60F; Olympus Co. Ltd, Tokyo, Japan). Minus a few exceptions, three microphotographs of transversal sections were taken for each stem and root sample with an APO (×5 or ×10) lens using a digital camera (Canon EOS 500D; Canon Inc., Tokyo, Japan) and some examples are shown in Fig. 1.

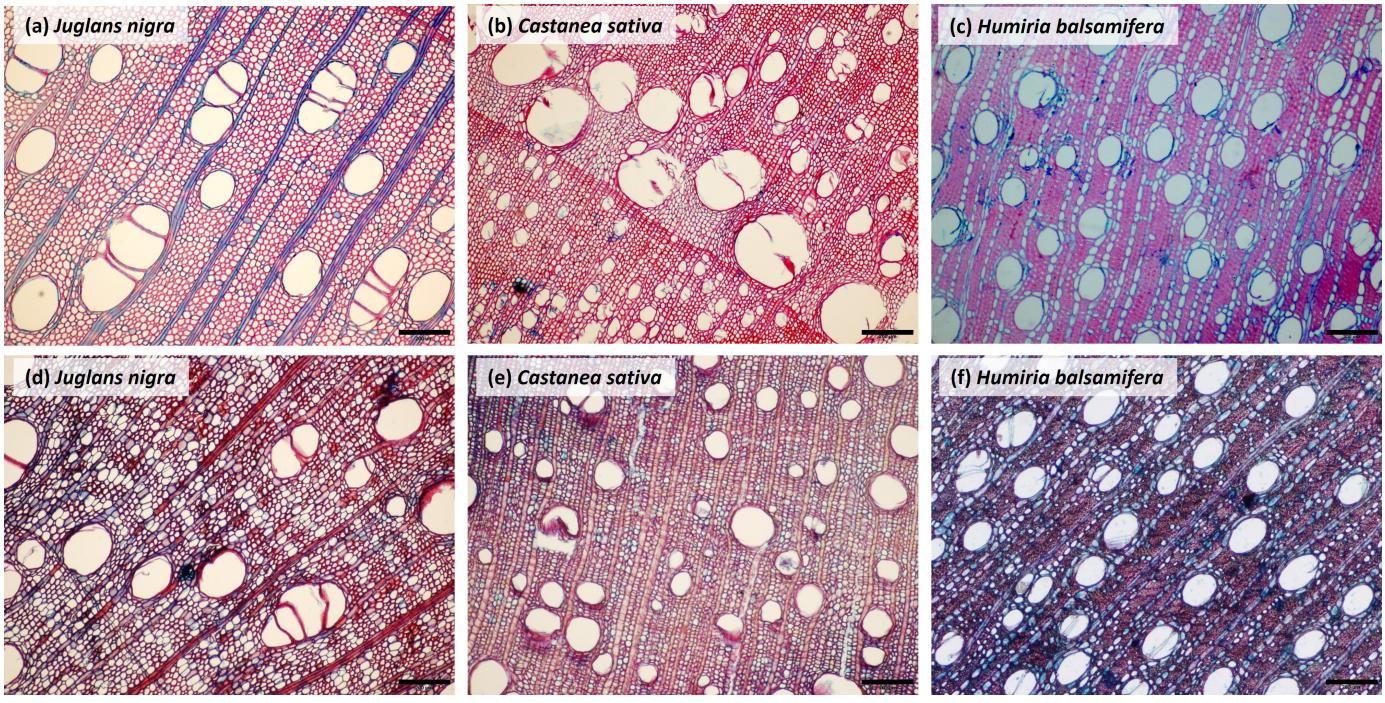


**Fig. 1** Light microscopy images of transversal sections of stems (a–c) and roots (d–f) of (a, d) *Juglans nigra*, (b, e) *Castanea sativa* and (c, f) *Humiria balsamifera*, illustrating the differences in xylem structure between the two organs. Bars, 200 µm.

Radial parenchyma and AP were manually coloured using Photoshop (Adobe Systems Incorporated, San Jose, CA, USA; see examples shown in Fig. S2). The proportions of RP (radial parenchyma area divided by xylem cross-sectional area, %) and AP (axial parenchyma area divided by xylem cross-sectional area, %) were estimated using ImageJ 1.52 software (https://imagej.nih.gov/ij/). The proportion of total RAP (i.e. the sum of RP and AP, %), was then calculated. Using the same image, we also determined VF (i.e. the total vessel area divided by xylem cross-sectional area). Some tree species can have fibre-tracheids and tracheids (FT; Table S2), but distinguishing these cell types from fibres in a transversal section is methodologically challenging (Baas & Carlquist, 1985; Wheeler *et al.*, 1989). In addition, FT are usually sparse with thick cell walls like fibres (Wheeler *et al.*, 1989; Ziemińska *et al.*, 2013). Therefore, we analysed fibres with FT together (FFT) in this study as also carried out by Kawai *et al.* (2021). Thus, the remaining tissue fraction was calculated as 1-RAP-VF. Vessel density (VD) is counted as the average number of conduits per $mm^2$ of xylem cross-section.

For all anatomical traits, we used the mean value calculated from the three images for subsequent statistical analyses.

**Hydraulic conductivity** Vessels were assumed elliptical in shape, and the diameter ($D_i$) of each vessel $i$ was estimated using Eqn 1 (Lewis, 1992):

$$D_i = \sqrt{\frac{2a^2b^2}{a^2+b^2}} \quad \text{Eqn 1}$$

where $a$ is the maximum diameter of a vessel and $b$ is the minimum diameter of a vessel. Vessel mean diameter ($D_m$) and the theoretical specific xylem hydraulic conductivity ($K_{th}$) were calculated based on the diameter of each vessel in the xylem cross-section (Fortunel *et al.*, 2014). $D_m$ was calculated as in Eqn 2:

$$D_m = \frac{\sum_{i=1}^{n} D_i}{n} \quad \text{Eqn 2}$$

$K_{th}$ was calculated using Hagen–Poiseuille equation (Tyree & Ewers, 1991) as in Eqn 3:

$$K_{th} = \frac{\pi\rho \sum_{i=1}^{n} D_i^4}{128\eta A_s} \quad \text{Eqn 3}$$

where $\rho$ is the density of water (998.2 kg $m^{-3}$ at 20°C), $\eta$ is the water viscosity ($1.002 \times 10^{-9}$ MPa s at 20°C) and $A_s$ is the xylem cross-sectional area which measured directly with ImageJ in the microphotograph.

The $K_{th}$ calculated according to Hagen–Poiseuille's law is thought to be an overestimate relative to the actual hydraulic conductivity due to the uncertain variation of the pit membrane and vessel length inside the tree (Loepfe *et al.*, 2007). However, there is empirical evidence showing that the relationship between these anatomical-based estimates and actual hydraulic measurements tends to be conserved across species (Sperry *et al.*, 2005).

**Wood density** The outer bark was removed on one stem and one root sample from each tree. Wood density was then measured by soaking samples in water for 24 h. The saturated volume was determined using the water displacement method (Pérez-Harguindeguy *et al.*, 2016). After determining the saturated volume, samples were dried in a well-ventilated oven at 105°C for up to 72 h and then the dry mass (DM) was weighed. Wood density used here is defined as oven-dry mass divided by saturated volume (Williamson & Wiemann, 2010).

**NSC content** Immediately on returning to the laboratory (on the same day the samples were collected), samples were heated in a microwave oven (90 s at 700 W) to stop enzymatic activity (Popp *et al.*, 1996) and then oven-dried at 40°C until a constant weight was obtained. Dried samples were ground into powder using a ball mill (Retsch MM400; Retsch, Haan, Germany), and the ground samples were stored in sealed plastic tubes until analysis. Due to the large number of samples ($n = 360$), we used the near-infrared spectroscopy (NIRS; Batten *et al.*, 1993) method to develop a model for predicting NSC contents in different organs (Zhang *et al.*, 2022a). The NIRS method has been used successfully in plant ecology for predicting NSC content in different tissue types of a broad range of tree species (Ramirez *et al.*, 2015; Rosado *et al.*, 2019).

As this study is part of a larger study, where NIRS was used to develop a model for predicting NSC in organs of 90 tree species (Zhang *et al.*, 2022a), we were able to create robust models using this larger dataset. First, 113 samples of stem and 140 samples of root were selected, for which values represented a broad range of data. Soluble sugars (SS) were extracted from 10 to 15 mg powder mixed in with 0.5 ml of 80% ethanol and incubated for 20 min at 80°C. The extraction was repeated twice and the three supernatants were collected in a tube and dried under vacuum (Refrigerated CentriVap Vacuum Concentrators, Labconco, Kansas City, MO, USA). The resulting soluble sugar extract was solubilized in 1.5 ml ultrapure water by sonication and agitation and then stored at −20°C. Total SS content was determined by a spectrophotometer at 620 nm (UV–visible DU 640 B; Beckman Coulter, Brea, CA, USA) using anthrone reagent and glucose as standard (Van Handel, 1965). Starch was extracted from the dried pellets in 1.5 ml of 0.2 M KOH solution incubated for 20 min at 80°C. Then, hydrolysis of starch into glucose was carried out in 0.1 M sodium acetate buffer solution at pH 4.75 with amyloglucosidase (EC 3.2.1.3. from *Aspergillus niger* Sigma A1602). The obtained glucose was determined colorimetrically using an enzymatic glucose oxidase (EC 1.1.3.4; Sigma G6125)/peroxidase (EC 1.11.1.7; Sigma P8125) and *O*-dianisidine dihydrochloride (Sigma D3252) reagent. After 10 min, 6N hydrochloric acid was added and absorbance was measured at 530 nm, using glucose as a standard (Chow & Landhäusser, 2004). SS and starch contents were expressed as mg $g^{-1}$ DM and their sum is referred to as the total NSC content.

Then, near-infrared spectra were obtained for all ground samples previously stabilized in a conditioning room at a temperature of 20 ± 2°C and air humidity of 65 ± 5%. A Bruker Vector 22/N spectrometer (Bruker, Burladingen, Germany) was used in reflectance mode. Data were measured for wavelengths between 1000 and 2500 nm with a resolution of 3 nm. The spectra set was thus composed by 501 wavelengths of reflectance values. NIRS spectra were first transformed (Naes *et al.*, 2004) with a standard normal variate (SNV) correction to reduce the effect of irregularities of surface and the intraspectrum variability (correction of the light dispersion). The second derivative was then computed using the algorithm of Savitzky and Golay (1964). The use of this derivative allowed for separating peaks that overlap and for correcting the baseline deviation of spectra and the range of NIRS values was examined.

Partial least squares regression (PLSR) was used to develop calibrations for the predictions of SS and starch content for stem and root samples separately (Zhang *et al.*, 2022a). The calibration $R^2$, standard error and root mean square error of cross-validation values are shown in Table S3.

### Statistical analysis

In this study, the minimum, maximum, mean, standard deviation and quartile coefficient of dispersion (QCD) of each trait were calculated. The data were transformed using natural log for all traits to homogenized variance. We used linear mixed models to test the effects of organs (stem and root) and climates (temperate, Mediterranean and tropical) on wood traits. We included organs, climates and their interactions as fixed effects. Species were introduced in models as random effects to account for pseudo-replicates. Tukey honestly significant differences (HSD) *post hoc* tests were also performed to identify variation between organs and among climates.

We used the standardized major axis (SMA) regression method (Warton *et al.*, 2006) to determine the scaling relationships among the wood traits across all species and among climates in (i) stems and (ii) roots. We also performed phylogenetic generalized least squares (PGLS) to investigate the influence of phylogenetic trends on wood trait associations with all species pooled together. We constructed a phylogenetic tree (Fig. S3) with all 60 species using the R package V.PhyloMaker (Jin & Qian, 2019), with the GBOTB phylogeny as the backbone (Smith and Brown, 2018). All species names were confirmed by the World Flora Online (http://www.worldfloraonline.org/). A Mantel test was performed to compare the pairwise wood trait correlation matrices between Pearson's test with and without phylogenetically independent contrasts (PICs). We also calculated Blomberg's *K*-value to evaluate the strength of phylogenetic signals for each trait (Blomberg *et al.*, 2003). In order to infer the potential connections between all wood traits, we also conducted a simple structural equation model (SEM) based on our hypotheses. The overall model fit was assessed with several tests, including a non-significant chi-squared ($\chi^2$) test ($P > 0.05$), a comparative fit index (CFI > 0.95) and a standardized root mean square residual (SRMR < 0.08; Malaeb *et al.*, 2000; Ali *et al.*, 2016).

All statistical analyses were performed in R v.4.0.2 (R Development Core Team, 2020), using the packages VEGAN (Dixon, 2003), APE (Paradis *et al.*, 2004), PICANTE (Kembel *et al.*, 2010), LAVAAN (Rosseel, 2012) and SMATR (Warton *et al.*, 2012).

## Results

### Patterns of wood traits in stem and root across 60 tree species

Across the 60 tree species, all wood traits showed marked interspecific variation (Figs S4, S5; Table 1). VD was the most variable trait in stems, ranging from 1.3 to 451.77 n mm$^{-2}$ with a QCD of 0.77, and $K_{th}$ was the most variable trait in roots, ranging from 0.45 to 459.18 kg m$^{-1}$ MPa$^{-1}$ s$^{-1}$ with a QCD of 0.72. The proportion of FFT and WD showed relatively small interspecific variation. In stem, FFT ranged from 0.47 to 0.88 with a QCD of 0.07 and for roots, FFT ranged from 0.27 to 0.88 with a QCD of 0.10 (Table 1). In stems, WD ranged from 0.24 to 0.85 g cm$^{-3}$ with a QCD of 0.14 and in roots, from 0.23 to 0.88 g cm$^{-3}$ with a QCD of 0.16 (Table 1). Generally, organ type had a greater effect on traits than the effect of climate: WD, FFT, VF, VD and $K_{th}$ were all significantly greater in stems than in roots, while AP, RP, RAP, SS, starch and NSC were all significantly lower in stems than in roots (Tables 1, 2).

The stem fibre fraction was lowest in temperate species and highest in tropical species, while no significant difference was found among climates for FFT in roots (Fig. 2a). The VF in both stems and roots was greatest in temperate species and lowest in tropical species (Fig. 2b). RAP and AP in both stems and roots were lowest in temperate species, whereas RP was the greatest in the stem of Mediterranean species, but did not vary in roots among the three climates (Figs 2c, S6a,b). Temperate species had lower WD in both stems and roots compared with Mediterranean and tropical species (Fig. 2d). The $K_{th}$ of both stems and roots was lower in Mediterranean species than in temperate and tropical species (Fig. 2e). Mediterranean species had more stem SS but less stem starch compared with temperate and tropical species, while stem NSC were not significantly different. However, tropical species possessed lower SS, starch and NSC contents in roots compared with temperate and Mediterranean species (Figs 2f, S6e,f).

### Independent trade-offs among wood cell types and functions in stem and root

Clear and strong trade-offs among cellular fractions were found in both stems and roots. VFs and RAP were significantly and negatively related to FFT, and RAP was also negatively correlated with VF in both stems and roots across all species (Figs 3a–c, 4a–c). However, the trade-offs among functions were complex. $K_{th}$ was negatively associated with WD, while no overall significant relationships between NSC and WD were found in either stem or root (Figs 3d,e, 4d,e). Interestingly, NSC was significantly and positively associated with $K_{th}$ in stem, whereas in roots, a negative relationship was found between NSC and $K_{th}$

**Table 1** Stem and root wood traits from 180 individual trees across 60 species.

| | | | Stem | | | | | Root | | | | |
|---|---|---|---|---|---|---|---|---|---|---|---|---|
| Trait | Abbrev. | Unit | Min | Max | Mean | SD | QCD | Min | Max | Mean | SD | QCD |
| Fibre with fibre-tracheids and tracheids fraction | FFT | – | 0.47 | 0.88 | 0.69 | 0.08 | 0.07 | 0.27 | 0.88 | 0.67 | 0.11 | 0.10 |
| Vessel fraction | VF | – | 0.02 | 0.39 | 0.13 | 0.07 | 0.41 | 0.02 | 0.33 | 0.11 | 0.07 | 0.42 |
| Vessel mean diameter | $D_m$ | μm | 16.43 | 216.36 | 75.43 | 41.72 | 0.37 | 20.00 | 218.32 | 73.74 | 34.02 | 0.32 |
| Vessel density | VD | n mm$^{-2}$ | 1.30 | 451.77 | 57.96 | 71.01 | 0.77 | 2.30 | 270.51 | 33.71 | 33.10 | 0.61 |
| Radial parenchyma fraction | RP | – | 0.04 | 0.29 | 0.13 | 0.05 | 0.30 | 0.05 | 0.37 | 0.14 | 0.06 | 0.28 |
| Axial parenchyma fraction | AP | – | 0.01 | 0.21 | 0.05 | 0.04 | 0.41 | 0.01 | 0.46 | 0.08 | 0.08 | 0.55 |
| Total parenchyma fraction | RAP | – | 0.05 | 0.39 | 0.18 | 0.06 | 0.24 | 0.07 | 0.65 | 0.22 | 0.10 | 0.28 |
| Wood density | WD | g cm$^{-3}$ | 0.24 | 0.85 | 0.56 | 0.12 | 0.14 | 0.23 | 0.88 | 0.51 | 0.13 | 0.16 |
| Specific xylem hydraulic conductivity | $K_{th}$ | kg m$^{-1}$ MPa$^{-1}$ s$^{-1}$ | 0.81 | 460.05 | 48.47 | 73.53 | 0.69 | 0.45 | 459.18 | 37.11 | 52.77 | 0.72 |
| Soluble sugars content | SS | mg g$^{-1}$ | 1.22 | 43.35 | 16.38 | 7.98 | 0.35 | 2.84 | 106.37 | 29.91 | 16.99 | 0.35 |
| Starch content | ST | mg g$^{-1}$ | 0.38 | 110.93 | 32.37 | 20.25 | 0.42 | 7.15 | 360.26 | 105.96 | 67.60 | 0.48 |
| Total NSC content | NSC | mg g$^{-1}$ | 7.58 | 120.91 | 49.06 | 22.61 | 0.32 | 21.34 | 376.39 | 135.12 | 74.25 | 0.40 |

Abbrev., abbreviation; Min, minimum; Max, maximum; NSC, nonstructural carbohydrates; QCD, quartile coefficient of dispersion.

**Table 2** Effects of organ and climate on the wood traits analysed using linear mixed model.

| | Organ | | | Climate | | | Organ × Climate | | |
|---|---|---|---|---|---|---|---|---|---|
| Traits | df | *F* | *P* | df | *F* | *P* | df | *F* | *P* |
| FFT | 1 | 12.52 | < 0.001*** | 2 | 0.51 | > 0.05 | 2 | 16.96 | < 0.001*** |
| VF | 1 | 15.75 | < 0.001*** | 2 | 9.70 | < 0.001*** | 2 | 7.99 | < 0.001*** |
| $D_m$ | 1 | 1.24 | > 0.05 | 2 | 25.40 | < 0.001*** | 2 | 27.79 | < 0.001*** |
| VD | 1 | 24.11 | < 0.001*** | 2 | 30.55 | < 0.001*** | 2 | 48.14 | < 0.001*** |
| RP | 1 | 9.19 | < 0.01** | 2 | 1.54 | > 0.05 | 2 | 0.05 | > 0.05 |
| AP | 1 | 49.77 | < 0.001*** | 2 | 5.96 | < 0.01** | 2 | 15.03 | < 0.001*** |
| RAP | 1 | 53.31 | < 0.001*** | 2 | 1.86 | > 0.05 | 2 | 9.25 | < 0.001*** |
| WD | 1 | 48.87 | < 0.001*** | 2 | 4.57 | < 0.05* | 2 | 5.35 | < 0.01** |
| $K_{th}$ | 1 | 11.59 | < 0.001*** | 2 | 4.80 | < 0.05* | 2 | 1.96 | > 0.05 |
| SS | 1 | 217.59 | < 0.001*** | 2 | 21.78 | < 0.001*** | 2 | 7.10 | < 0.001*** |
| ST | 1 | 320.96 | < 0.001*** | 2 | 2.28 | > 0.05 | 2 | 28.13 | < 0.001*** |
| NSC | 1 | 524.27 | < 0.001*** | 2 | 5.55 | < 0.01** | 2 | 23.08 | < 0.001*** |

AP, axial parenchyma; df, degree of freedom; $D_m$, vessel mean diameter; *F*, Fisher value; FFT, fibre with fibre-tracheids and tracheids; $K_{th}$, theoretical specific xylem hydraulic conductivity; NSC, nonstructural carbohydrates; RAP, radial and axial parenchyma; RP, radial parenchyma; SS, soluble sugars; ST, starch; VD, vessel density; VF, vessel fraction; WD, wood density. *P* indicates the significance level. *, $P < 0.05$; **, $P < 0.01$; ***, $P < 0.001$.

(Figs 3f, 4f). Wood density was not significantly associated with FFT and $K_{th}$ was positively associated with VF in both stems and roots (Figs 3g,h, 4g,h). There was a positive relationship between NSC and RAP across the stems of all species, but not in roots (Figs 3i, 4i).

Relationships between wood traits varied between climates. Basically, trade-offs among cellular fractions of stem and root wood were generally observed within climates (Figs 3a–c, 4a–c; Tables S4, S5). However, the significant relationships disappeared in some climates when referring to the traits that acted as proxies for functions. For example, there were no significant relationships between stem WD and $K_{th}$ within a given climate and no significant relationship was found between root WD and $K_{th}$ in tropical species (Figs 3d, 4d; Tables S4, S5). Positive relationships between WD and NSC for both stems and roots were only found in Mediterranean species (Figs 3e, 4e; Tables S4, S5). Similarly, stem $K_{th}$ was only associated with stem NSC in temperate species and no significant correlation was found between root $K_{th}$ and NSC in any climate (Figs 3f, 4f; Tables S4, S5).

The phylogenetic analysis showed similar results to the cross-species analysis regarding trait relationships (Tables 3, S6). However, many traits had significant phylogenetic signals, including WD, RP, RAP, FFT, VF, $D_m$ and VD in stems and AP, RP, RAP, VD, SS, starch and NSC in roots (Table S7).

The result of the SEM confirmed that there were allocation trade-offs among cell fractions in both stems and roots and, as in

New Phytologist

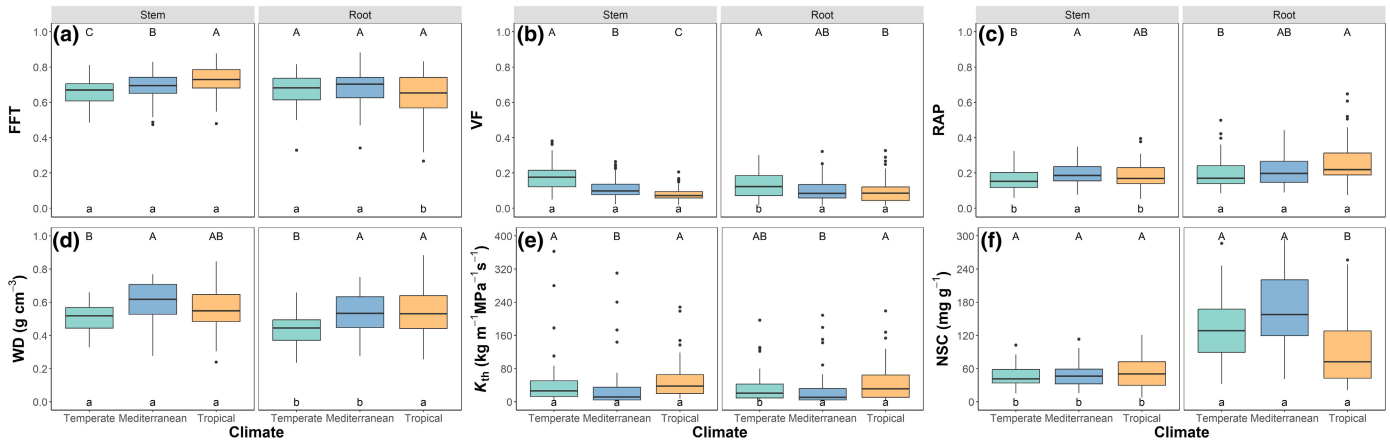


**Fig. 2** Boxplots of (a) fibre (FFT), (b) vessel (VF) and (c) radial and axial parenchyma (RAP) fractions in stem (left panel) and root (right panel) xylem for 60 species across from temperate, Mediterranean and tropical climates. The functions commonly associated with these anatomical traits are (d) mechanical integrity represented by wood density (WD), (e) water transport represented by theoretical specific xylem hydraulic conductivity ($K_{th}$) and (f) storage of nonstructural carbohydrates (NSC). The line in the box indicates the median; the whiskers above and below the box indicate the 75$^{th}$ and 25$^{th}$ percentiles; the points indicate outlier values. Different uppercase letters indicate significant differences between climates for a given xylem trait in the same organ. Different lowercase letters indicate significant differences between organs for a given xylem trait in the same climate. Colours indicate three climates: light green, temperate climate; light blue, Mediterranean climate; orange, tropical climate.

the previous analyses, the relationships between $K_{th}$ and NSC were contrasting (Fig. 5). The framework constructed by the SEM showed that WD was not associated with NSC in either stems or roots and negative relationships between WD and $K_{th}$ were found in both stems and roots (Fig. 5). Additionally, RAP and FFT were strongly and positively associated with WD in both stems and roots (Fig. 5). There were significant relationships among cell types in stem and root wood for species in most climates, but the trade-off among functions was complex and differed across climates (Fig. S7).

## Discussion

### Variations in wood traits in stems and roots across climates

Corroborating our H1, we showed that the total parenchyma and AP fractions were more abundant in roots than stems when all species pooled together, providing roots with a greater capacity to store NSC. In agreement with Morris *et al.* (2016), we also found that the total parenchyma fraction was greater in tropical than in temperate species, which was mainly due to the increase in AP rather than RP. Tropical species had fewer but larger vessels in both stems and roots, with greater hydraulic conductivity. By contrast, Mediterranean species had the lowest hydraulic conductivity in both stem and root wood, due mainly to narrower vessels, even though vessel density was greater than in trees from other climates. Species from water-limited environments, such as the Mediterranean area, are characterized by high embolism resistance and low hydraulic transport efficiency (Maherali *et al.*, 2004; Liu *et al.*, 2019). The climate in tropical French Guiana is relatively moist and warm; therefore, the risk of drought-induced embolism is negligible (Ziegler *et al.*, 2019), but there may be exceptions in the case of an extreme drought (Rowland *et al.*, 2015; Fontes *et al.*, 2020), and as vessel size is not constrained, it can be increased to enhance water uptake. Similarly, freeze–thaw-induced xylem embolism is less likely to occur in warmer tropical forests than in temperate tree species or some Mediterranean tree species that are more susceptible to freeze–thaw stress (Sperry & Sullivan, 1992; Hacke *et al.*, 2017). Therefore, wider vessels associated with higher hydraulic conductivity are again more likely to occur in tropical systems.

Wood density in both stems and roots of temperate species was lower than that in species from other climates. However, the variability in data from tropical species was high and the range of density values was also large, as also found by Wiemann and Williamson (2002). Root NSC content was always higher than in the stem, as also found by Martínez-Vilalta *et al.* (2016), Smith *et al.* (2018) and Furze *et al.* (2020). A high NSC content in roots allows for fast root growth in the spring, improving the supply of water and nutrients necessary for budburst or leafing out (Abramoff & Finzi, 2015). Mediterranean species had more NSC in roots, which could aid resprouting and the recovery of hydraulic conductivity if embolism occurs (Yoshimura *et al.*, 2016; Kono *et al.*, 2019), especially during long, dry periods. Tropical species had the least NSC in roots, possibly because they allocate more carbon for growth and respiration throughout the longer growing season, resulting in a lower overall NSC (Körner, 2003; Martínez-Vilalta *et al.*, 2016). In agreement with Martínez-Vilalta *et al.* (2016), we did not find a significant difference among the three climates with regard to total NSC in stems.

### Trade-offs among cell types do not reflect functional trade-offs in stems and roots

Clear allocation trade-offs among cell types were found in both stems and roots across all species, reflecting spatial constraints (Pratt & Jacobsen, 2017) and corroborating our H2. Fibres occupied the most space, at the expense of vessels or parenchyma.

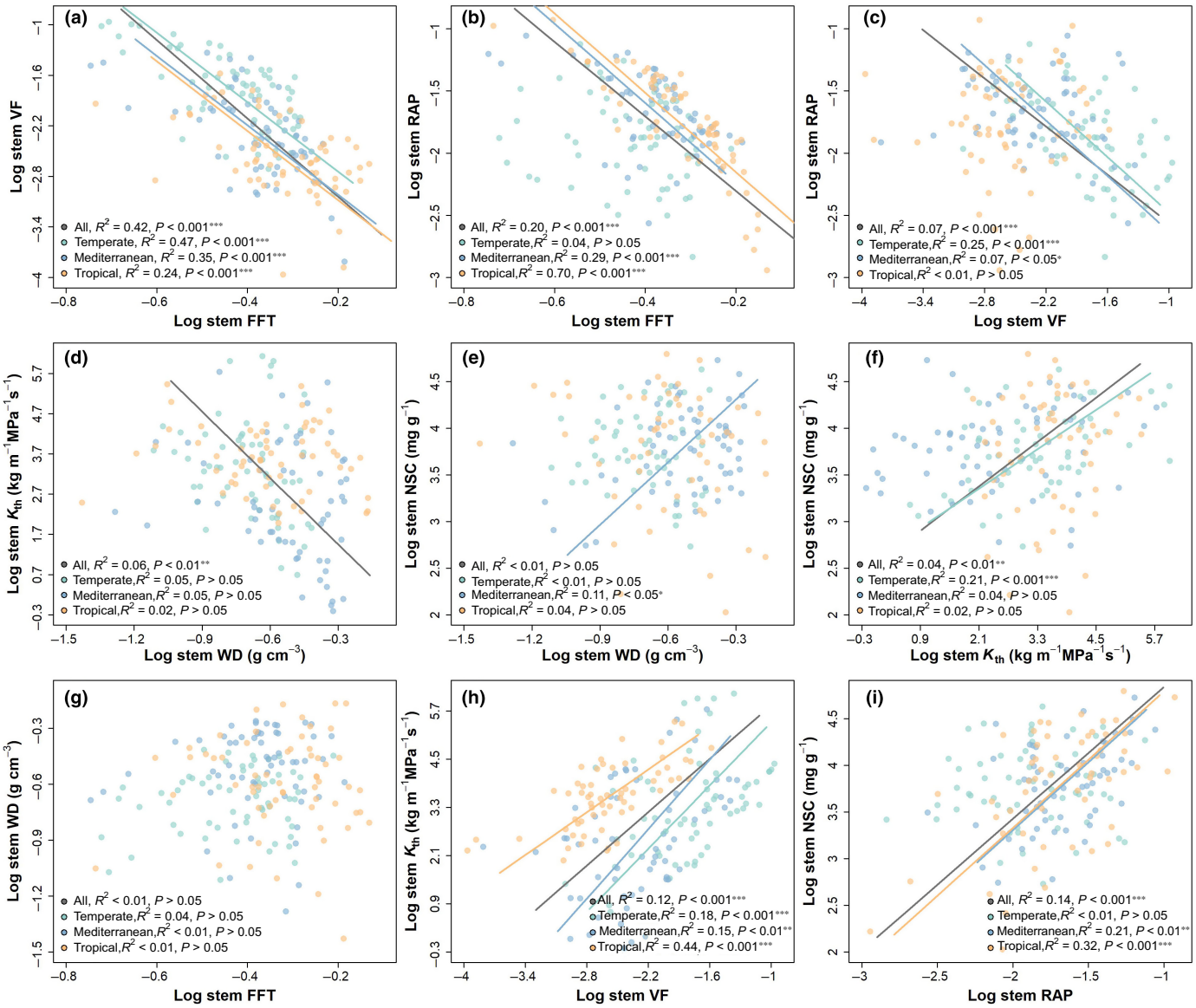


**Fig. 3** Standardized major axis (SMA) regressions among log stem anatomical traits and the proxies of functions commonly associated with these anatomical traits, for 60 species in temperate, Mediterranean and tropical climates. Relationships between (a) Vessel fraction (VF) and fibre fraction (FFT), (b) radial and axial parenchyma fraction (RAP) and FFT, (c) RAP and VF, (d) theoretical specific xylem hydraulic conductivity ($K_{th}$) and wood density (WD), (e) nonstructural carbohydrates (NSC) and WD, (f) NSC and $K_{th}$, (g) WD and FFT, (h) $K_{th}$ and VF and (i) NSC and RAP. Significant regression lines, $R^2$ and $P$-values are shown. Asterisks indicate the degree of significant relationships. Grey lines represent associations across all species. Different colours indicate tree species from different climates: light green, temperate species; light blue, Mediterranean species; orange, tropical species. Model parameters are reported in Supporting Information Table S4.

However, functions did not exhibit the same patterns and were complex and diverse, which is in agreement with our H3. We found negative relationships between WD and hydraulic conductivity in both stems and roots across all species pooled together, implying that there is a trade-off between mechanical integrity and hydraulic conductivity, as also found by several authors (Smith & Ennos, 2003; Christensen-Dalsgaard *et al.*, 2007a,b; McCulloh *et al.*, 2011; Janssen *et al.*, 2020). Wood density has been used as a proxy for the hydraulic properties of stems (Markesteijn *et al.*, 2011; Hoeber *et al.*, 2014), as hydraulic conductivity is proportional to vessel diameter to the fourth power, suggesting that species with wide vessels have high water transport efficiency and reduced WD due to a lower fibre fraction. Similarly, dense wood has greater cell packing, with narrow vessel lumina (Zanne *et al.*, 2010; Markesteijn *et al.*, 2011). It is assumed that dense tissues reduce hydraulic efficiency because of narrower and potentially shorter vessels, as well as thicker walls that will increase the path length through the pits where sap flows between narrow vessels (Lens *et al.*, 2011; Pratt *et al.*, 2021a). However, this negative relationship between WD and hydraulic conductivity does not seem to be universally valid as other studies failed to find it (Pratt *et al.*, 2007; Martínez-Cabrera *et al.*, 2009; Poorter *et al.*, 2010; Schuldt *et al.*, 2013; Fortunel *et al.*, 2014). A possible explanation may be that other properties could drive WD, such as fibre wall

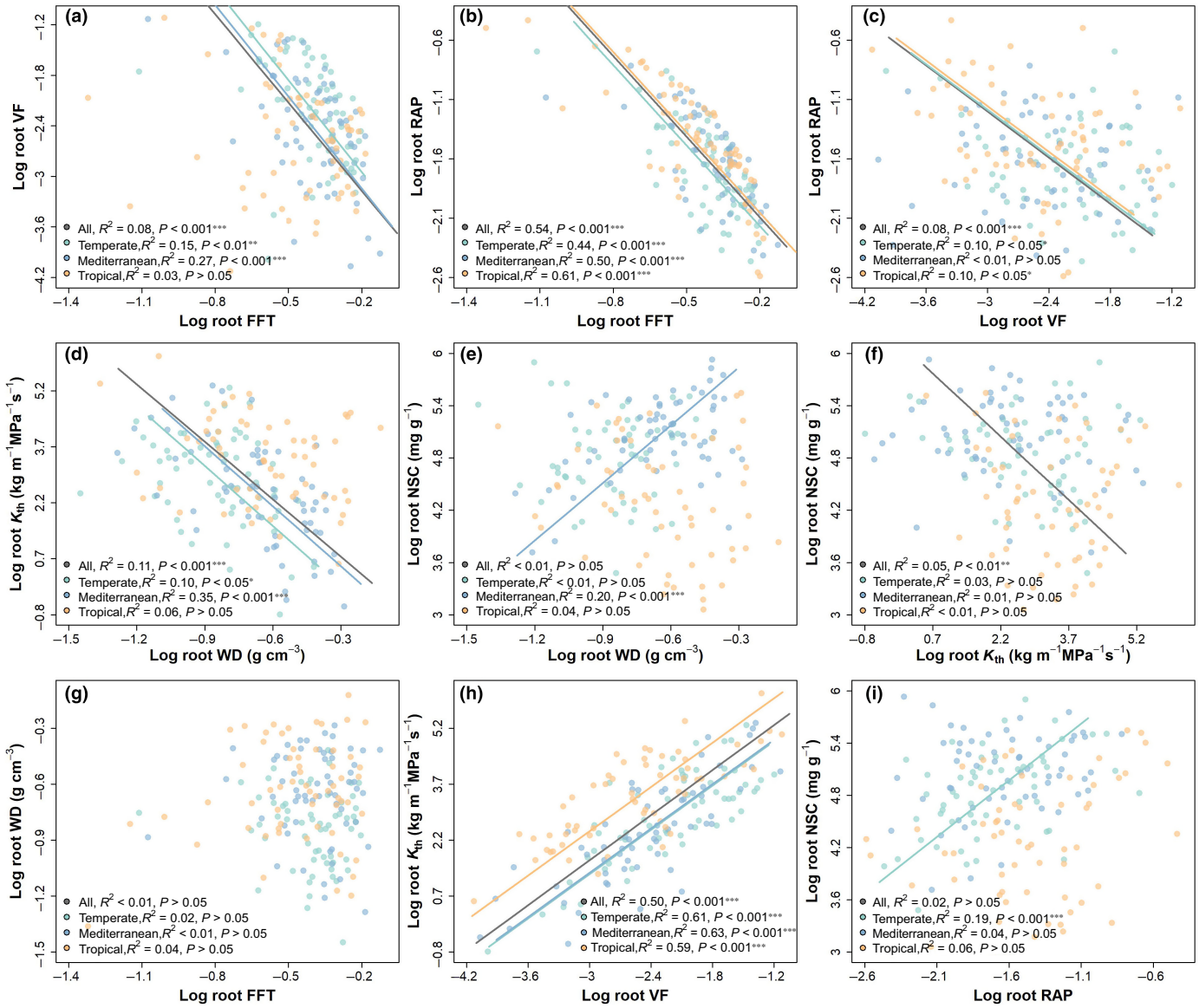


**Fig. 4** Standardized major axis (SMA) regressions among log root anatomical traits and the proxies of functions commonly associated with these anatomical traits, for 60 species in temperate, Mediterranean and tropical climates. Relationships between (a) Vessel fraction (VF) and fibre fraction (FFT), (b) radial and axial parenchyma fraction (RAP) and FFT, (c) RAP and VF, (d) theoretical specific xylem hydraulic conductivity ($K_{th}$) and wood density (WD), (e) nonstructural carbohydrates (NSC) and WD, (f) NSC and $K_{th}$, (g) WD and FFT, (h) $K_{th}$ and VF and (i) NSC and RAP. Significant regression lines, $R^2$ and $P$-value are shown. Asterisks indicate the degree of significant relationships. Grey lines represent associations across all species. Different colours indicate tree species from different climates: light green, temperate species; light blue, Mediterranean species; orange, tropical species. Model parameters are reported in Supporting Information Table S5.

thickness, but do not directly affect hydraulic conductivity (Ziemińska *et al.*, 2013; Hoeber *et al.*, 2014; Badel *et al.*, 2015). Previous studies have also shown that although WD was not related to total fibre fraction, it was positively correlated with fibre wall fraction and negatively with fibre lumen fraction (Jacobsen *et al.*, 2005; Ziemińska *et al.*, 2013; Janssen *et al.*, 2020), properties that were not measured in our study.

We found that WD was positively correlated with total parenchyma fraction, suggesting that WD could be a good predictor of NSC storage capacity. However, though RAP fraction was positively correlated with NSC content, we found no correlation between WD and NSC in either stem or root. The positive relationship between WD and parenchyma content is well documented, as wood with a high proportion of AP usually has fibres with narrow lumina (Woodrum *et al.*, 2003; Martínez-Cabrera *et al.*, 2009; Rana *et al.*, 2009; Zhang *et al.*, 2022b). Additionally, RP can be strongly lignified and high lignin content increases WD (Harada & Wardrop, 1960; Zheng *et al.*, 2016). Also, we expressed NSC content per unit of mass, not sapwood volume. Comparisons of NSC concentrations should also account for changes in the density of structural compounds, which can obscure differences in effective compound concentration per cell unit (Hoch *et al.*, 2002). Overall, our results indicate that WD is a poor predictor of the NSC content in trees.

**Table 3** Phylogenetic correlations based on phylogenetic generalized least squares (PGLS) among wood traits of stem and root across 60 species.

| | Stem | | Root | |
|---|---|---|---|---|
| Models | $R^2$ | $P$ | $R^2$ | $P$ |
| VF ~ FFT | 0.32 | < 0.001*** | 0.09 | < 0.05* |
| RAP ~ FFT | 0.29 | < 0.001*** | 0.62 | < 0.001*** |
| RAP ~ VF | 0.12 | < 0.01** | 0.06 | > 0.05 |
| $K_{th}$ ~ WD | 0.07 | < 0.05* | 0.14 | < 0.001*** |
| NSC ~ WD | 0.01 | > 0.05 | 0.01 | > 0.05 |
| NSC ~ $K_{th}$ | 0.04 | > 0.05 | 0.07 | < 0.05* |
| WD ~ FFT | 0.01 | > 0.05 | 0.01 | > 0.05 |
| $K_{th}$ ~ VF | 0.09 | < 0.05* | 0.54 | < 0.001*** |
| NSC ~ RAP | 0.25 | < 0.001*** | 0.08 | < 0.05* |

FFT, fibre with fibre-tracheids and tracheids; $K_{th}$, theoretical specific xylem hydraulic conductivity; NSC, non-structural carbohydrates; RAP, radial and axial parenchyma; VF, vessel fraction; WD, wood density.
$P$ indicates the significance level. *, $P < 0.05$; **, $P < 0.01$; ***, $P < 0.001$.

In agreement with our H3, we found that NSC content was positively associated with hydraulic conductivity in stems, but negatively in roots. Stem wood needs high levels of NSC to allow for the production of new and large earlywood vessels, especially in ring-porous species. The most common species that have ring-porous stems rarely refill winter-embolized vessels and mostly rely on new sapwood growth by cambial activity in the earlywood to carry water during the growing season (Hacke & Sperry, 2001; Barbaroux & Bréda, 2002), which requires the use of local or imported NSCs and represents a medium to long-term strategy for hydraulic recovery. Lateral roots are usually diffuse-porous with more numerous vessels throughout the xylem. Previous studies demonstrated that roots are more vulnerable to xylem cavitation than stems (Sperry & Ikeda, 1997; Maherali *et al.*, 2006; Hacke & Jansen, 2009; Domec *et al.*, 2010) and the embolism repair or vessel refilling may be dependent on the role of SS and parenchyma cells surrounding vessels (Secchi *et al.*, 2017; Tomasella *et al.*, 2020). However, recent studies have shown that coarse roots are not highly vulnerable to xylem embolism as commonly believed (Peters *et al.*, 2020; Wu *et al.*, 2020; Lübbe et al., 2022). In addition, even if root embolism occurs (especially for freeze–thaw-induced xylem embolism), the repair of embolism may probably depend on root pressure (the positive pressure resulting from osmolyte accumulation in root tissues; Wegner, 2014) rather than osmotic regulation achieved by SS (Wang *et al.*, 2022). Thus, the recovery of hydraulic conductivity is less dependent on stored carbon. This opposing strategy may also be related to the different functions performed by RAP in roots and stems (Zheng & Martínez-Cabrera, 2013; Secchi *et al.*, 2017; Aritsara *et al.*, 2021). In agreement with Morris *et al.* (2018), a large AP fraction was associated with wider vessels, consistent with a potential role in water transport. By contrast, RP was negatively correlated with hydraulic conductivity, demonstrating the functional differentiation of AP and RP in hydraulic efficiency (Zheng & Martínez-Cabrera, 2013). Also, AP may perform different functions in roots compared to stems, where it serves a role for hydraulic functioning, which could lead to different strategies between stems and roots.

## The impact of phylogeny and climate on structure–function relationships

Certain wood anatomical traits exhibited strong phylogenetic signals as also observed by Zheng *et al.* (2019), which supports the

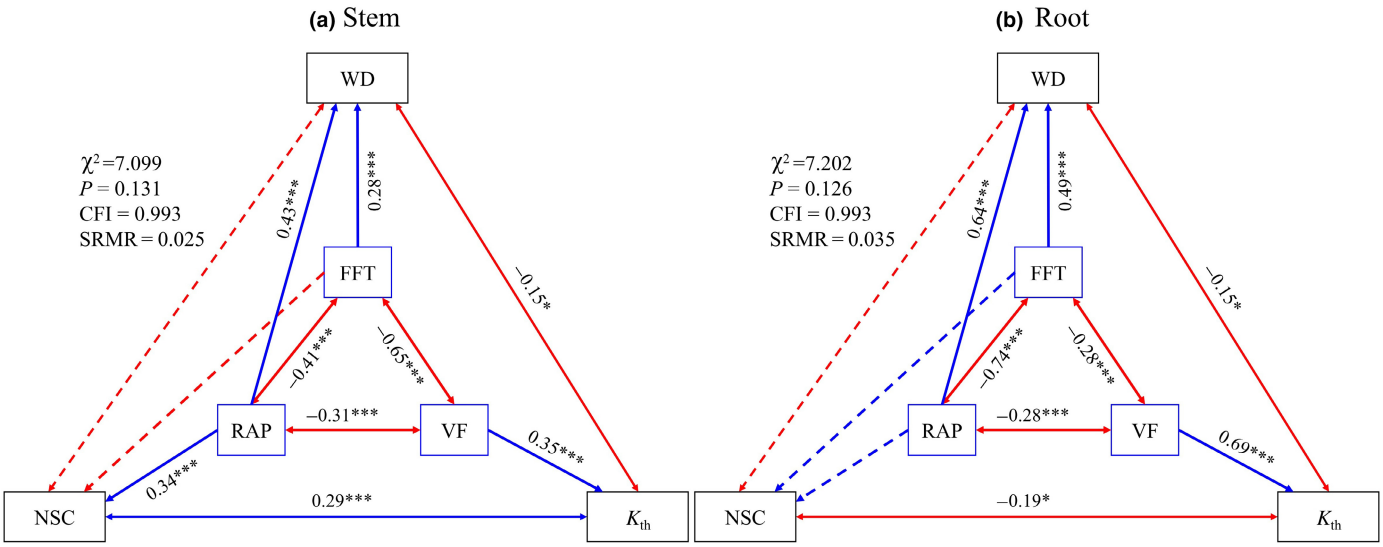


**Fig. 5** Structural equation model (SEM) for displaying trade-offs among cellular fractions and the functions commonly associated with these traits in stem (a) and root (b) xylem in 60 species across three climates. Anatomical traits (inner triangle) include fibre (FFT), vessel (VF) and radial and axial parenchyma (RAP) fractions. Functional traits (outer triangle) are mechanical integrity represented by wood density (WD), water transport represented by theoretical specific xylem hydraulic conductivity ($K_{th}$) and storage of nonstructural carbohydrates (NSC). Solid arrows represent significant paths ($P < 0.05$), while dashed arrows represent nonsignificant paths. The red lines indicate negative correlations, while the blue lines indicate positive correlations. For each path, the standardized regression coefficient is shown. Asterisks indicate the degree of significant relationships. Several model-fit statistics are shown, including chi-square ($\chi^2$), $P$-value, comparative fit index (CFI) and standardized root mean square residual (SRMR).

notion that wood anatomy is relatively conservative and largely determined by evolutionary history. However, our phylogenetic analysis showed the correlations between PGLS trait values were similar as those with raw trait values, suggesting that evolutionary histories cannot explain the associations among the traits we sampled, as also found by Pratt *et al.* (2021a). In addition, we found that the relationships among cell types exhibited strong trade-offs across species within each climate, although some relationships were only weakly correlated. This result means that the covariation among cell fractions is conserved and does not experience large fluctuations within a given climatic zone (Morris *et al.*, 2016; Pratt & Jacobsen, 2017). On the contrary, relationships among functions across species are complex and tend to vary among climates, which corroborates our H4. The reason may be that in different climates, WD can be influenced by other properties, such as fibre wall thickness, but hydraulic conductivity might not be directly affected by these properties (Ziemińska *et al.*, 2013; Hoeber *et al.*, 2014; Badel *et al.*, 2015). Additionally, NSC can show seasonal variation (Smith *et al.*, 2018; Furze *et al.*, 2020) and could be involved in the reversal of embolism, especially for trees growing in temperate regions that are susceptible to freeze–thaw-induced xylem embolism (Nardini *et al.*, 2011; Sala *et al.*, 2012).

### Caveats

Although cell types and functions in xylem are entwined and interconnected in a complex way, different cell types still have different functions. Tracheids, fibre-tracheids and fibres typically play different roles in the xylem, but are difficult to distinguish in transversal sections (Baas & Carlquist, 1985; Wheeler *et al.*, 1989). Analysing these three cells together in our study may ignore the role played by each cell type, thereby affecting the relationship between allocation and functional trade-offs. Therefore, more effort is required in future studies, especially with regard to distinguishing cell types, to improve our understanding of the relationships between cell type fractions and wood functions in trees. Living wood fibres that retain live protoplast for months or years are often overlooked cell types in structure and function studies, even though they are analogous in their function to AP strands (Fahn & Leshem, 1963; Yamada *et al.*, 2011). Living fibres are much more common than supposed, but they remain poorly understood because they are difficult to detect in fresh wood samples (Gregory, 1978). Further experimental work with improved techniques and methods on how or to what extent living fibres play a major role in xylem function will be important towards reaching this goal.

### Conclusion

We evaluated the coordination in wood structure and functions across 60 angiosperm tree species in three distinct climates. By examining the changes in wood design in stems and roots of the same individuals, we found that there were clear and strong trade-offs in carbon allocation among cell type fractions. However, the covariations among functions were more complex. We thus underline that trade-offs in carbon allocation do not necessarily reflect functional trade-offs in stems and roots. We further point out that although WD was negatively correlated with $K_{th}$, suggesting a trade-off between mechanical integrity and hydraulic conductivity, no relationship was observed between WD and NSC. Additionally, NSC storage capacity in stems was positively associated with hydraulic conductivity, but negatively in roots, demonstrating that there is also a difference in this functional relationship between stems and roots. Our study provides new insight into the structure and function of xylem within trees from diverse locations and helps us to better understand the behaviour of trees under global climate change and how they can cope with increasing drought events in the future.

## Acknowledgements

This study was supported by a grant from Investissement d'Avenir grants of the ANR, France (CEBA: ANR-10-LABX-25-01) and China Scholarship Council (CSC, no. 201806300029, for GZ). We are grateful to J. Cazal (INRAE), S. Nourissier-Mountou (CIRAD), N. Boutahar (CIRAD), M. Ramel (INRAE) and S. Fourtier (INRAE), for their help with field and laboratory work. We thank G. Derroire, A. Dourdain, C. Stahl and S. Coste for their aid with logistical arrangements at Paracou field station and at ECOFOG laboratory in French Guiana. The collecting of genetic resources in French Guiana was authorized by the French Government (APA no. 1371201). Thanks are due to managers of state-owned land for their collaboration and to Mr. and Mrs. R. Lecoustre and B. Dupin (Société Eco-Altitude) for permission to sample trees on private property. The authors would like to thank Prof. L. Poorter (Wageningen University and Research) for his help in the early discussions in the paper. The authors would like to thank SILVATECH (doi: 10.15454/1.5572400113627854E12) from UMR 1434 SILVA, 1136 IAM, 1138 BEF and 4370 EA LERMAB from the research centre INRAE Grand-Est Nancy for its contribution to NSC analyses. The SILVATECH facility is supported by the French National Research Agency through the Laboratory of Excellence ARBRE (ANR-11-LABX-0002-01).

## Competing interests

None declared.

## Author contributions

GZ and AS planned and designed the research. GZ, ZM, PM, JE, CF, PH, J-LM, JM-V and AS conducted fieldwork. GZ, LB, BG, AS and CF performed laboratory analyses. GZ, ZM and AS analysed the data. All the authors contributed critically to the drafts and gave final approval for publication.

## ORCID

Claire Fortunel https://orcid.org/0000-0002-8367-1605
Bastien Gérard https://orcid.org/0000-0003-3132-0552
Patrick Heuret https://orcid.org/0000-0002-7956-0451

Jean-Luc Maeght https://orcid.org/0000-0002-7292-1955
Pascale Maillard https://orcid.org/0000-0002-6088-8561
Zhun Mao https://orcid.org/0000-0001-8042-6316
Jordi Martínez-Vilalta https://orcid.org/0000-0002-2332-7298
Alexia Stokes https://orcid.org/0000-0002-2276-0911
Guangqi Zhang https://orcid.org/0000-0002-7151-2885

## Data availability

The data described in this paper are freely and openly accessed at Data INRAE at https://doi.org/10.57745/X6WW8A.

## References

**Abramoff RZ, Finzi AC. 2015.** Are above-and below-ground phenology in sync? *New Phytologist* **205**: 1054–1061.

**Ali A, Yan ER, Chen HYH, Chang SX, Zhao YT, Yang XD, Xu M-S. 2016.** Stand structural diversity rather than species diversity enhances aboveground carbon storage in secondary subtropical forests in Eastern China. *Biogeosciences* **13**: 4627–4635.

**Aritsara ANA, Razakandraibe VM, Ramananantoandro T, Gleason SM, Cao K-F. 2021.** Increasing axial parenchyma fraction in the Malagasy Magnoliids facilitated the co-optimisation of hydraulic efficiency and safety. *New Phytologist* **229**: 1467–1480.

**Baas P, Carlquist S. 1985.** A Comparison of the ecological wood anatomy of the floras of Southern California and Israel. *The IAWA Journal* **6**: 349–353.

**Baas P, Ewers FW, Davis SD, Wheeler EA. 2004.** Evolution of xylem physiology. In: Hemsley AR, Poole I, eds. *The evolution of plant physiology.* London, UK: Elsevier Academic Press, 273–295.

**Badel E, Ewers FW, Cochard H, Telewski FW. 2015.** Acclimation of mechanical and hydraulic functions in trees: impact of the thigmomorphogenetic process. *Frontiers in Plant Science* **6**: 266.

**Barbaroux C, Bréda N. 2002.** Contrasting distribution and seasonal dynamics of carbohydrate reserves in stem wood of adult ring-porous sessile oak and diffuse-porous beech trees. *Tree Physiology* **22**: 1201–1210.

**Batten GD, Blakeney AB, McGrath VB, Ciavarella S. 1993.** Non-structural carbohydrate: analysis by near infrared reflectance spectroscopy and its importance as an indicator of plant growth. *Plant and Soil* **155**: 243–246.

**Blomberg SP, Garland T, Ives AR. 2003.** Testing for phylogenetic signal in comparative data: behavioral traits are more labile. *Evolution* **57**: 717–745.

**Burgert I, Eckstein D. 2001.** The tensile strength of isolated wood rays of beech (*Fagus sylvatica* L.) and its significance for the biomechanics of living trees. *Trees* **15**: 168–170.

**Chave J, Coomes D, Jansen S, Lewis SL, Swenson NG, Zanne AE. 2009.** Towards a worldwide wood economics spectrum. *Ecology Letters* **12**: 351–366.

**Chen Z, Zhu S, Zhang Y, Luan J, Li S, Sun P, Wan X, Liu S. 2020.** Tradeoff between storage capacity and embolism resistance in the xylem of temperate broadleaf tree species. *Tree Physiology* **40**: 1029–1042.

**Choat B, Brodribb TJ, Brodersen CR, Duursma RA, López R, Medlyn BE. 2018.** Triggers of tree mortality under drought. *Nature* **558**: 531–539.

**Chow PS, Landhäusser SM. 2004.** A method for routine measurements of total sugar and starch content in woody plant tissues. *Tree Physiology* **24**: 1129–1136.

**Christensen-Dalsgaard KK, Ennos AR, Fournier M. 2007a.** Changes in hydraulic conductivity, mechanical properties, and density reflecting the fall in strain along the lateral roots of two species of tropical trees. *Journal of Experimental Botany* **58**: 4095–4105.

**Christensen-Dalsgaard KK, Fournier M, Ennos AR, Barfod AS. 2007b.** Changes in vessel anatomy in response to mechanical loading in six species of tropical trees. *New Phytologist* **176**: 610–622.

**Dixon P. 2003.** VEGAN, a package of R functions for community ecology. *Journal of Vegetation Science* **14**: 927–930.

**Domec J-C, Schäfer K, Oren R, Kim HS, McCarthy HR. 2010.** Variable conductivity and embolism in roots and branches of four contrasting tree species and their impacts on whole-plant hydraulic performance under future atmospheric $CO_2$ concentration. *Tree Physiology* **30**: 1001–1015.

**Fahn A. 1967.** *Plant anatomy.* Oxford, UK: Pergamon Press Ltd, 514.

**Fahn A, Leshem B. 1963.** Wood fibres with living protoplasts. *New Phytologist* **62**: 91–98.

**Felsenstein J. 1985.** Phylogenies and the comparative method. *The American Naturalist* **125**: 1–15.

**Fontes CG, Fine PVA, Wittmann F, Bittencourt PRL, Piedade MTF, Higuchi N, Chambers JQ, Dawson TE. 2020.** Convergent evolution of tree hydraulic traits in Amazonian habitats: implications for community assemblage and vulnerability to drought. *New Phytologist* **228**: 106–120.

**Fortunel C, Ruelle J, Beauchêne J, Fine PVA, Baraloto C. 2014.** Wood specific gravity and anatomy of branches and roots in 113 Amazonian rainforest tree species across environmental gradients. *New Phytologist* **202**: 79–94.

**Furze ME, Huggett BA, Chamberlain CJ, Wieringa MM, Aubrecht DM, Carbone MS, Walker JC, Xu X, Czimczik CI, Richardson AD. 2020.** Seasonal fluctuation of nonstructural carbohydrates reveals the metabolic availability of stemwood reserves in temperate trees with contrasting wood anatomy. *Tree Physiology* **40**: 1355–1365.

**Gregory RA. 1978.** Living elements of the conducting secondary xylem of sugar maple (*Acer saccharum* Marsh.). *IAWA Bulletin* **4**: 65–70.

**Grubb PJ. 2016.** Trade-offs in interspecific comparisons in plant ecology and how plants overcome proposed constraints. *Plant Ecology & Diversity* **9**: 3–33.

**Hacke UG, Jansen S. 2009.** Embolism resistance of three boreal conifer species varies with pit structure. *New Phytologist* **182**: 675–686.

**Hacke UG, Sperry JS. 2001.** Functional and ecological xylem anatomy. *Perspectives in Plant Ecology, Evolution and Systematics* **4**: 97–115.

**Hacke UG, Spicer R, Schreiber SG, Plavcová L. 2017.** An ecophysiological and developmental perspective on variation in vessel diameter. *Plant, Cell & Environment* **40**: 831–845.

**Harada H, Wardrop AB. 1960.** Cell wall structure of ray parenchyma cells of a softwood. *Journal of the Japan Wood Research Society* **6**: 34–41.

**Hoch G, Popp M, Körner C. 2002.** Altitudinal increase of mobile carbon pools in *Pinus cembra* suggests sink limitation of growth at the Swiss treeline. *Oikos* **98**: 361–374.

**Hoeber S, Leuschner C, Köhler L, Arias-Aguilar D, Schuldt B. 2014.** The importance of hydraulic conductivity and wood density to growth performance in eight tree species from a tropical semi-dry climate. *Forest Ecology and Management* **330**: 126–136.

**Jacobsen AL, Agenbag L, Esler KJ, Pratt RB, Ewers FW, Davis SD. 2007.** Xylem density, biomechanics and anatomical traits correlate with water stress in 17 evergreen shrub species of the Mediterranean-type climate region of South Africa. *Journal of Ecology* **95**: 171–183.

**Jacobsen AL, Ewers FW, Pratt RB, Paddock WA III, Davis SD. 2005.** Do xylem fibers affect vessel cavitation resistance? *Plant Physiology* **139**: 546–556.

**Janssen TAJ, Hölttä T, Fleischer K, Naudts K, Dolman H. 2020.** Wood allocation trade-offs between fibre wall, fibre lumen, and axial parenchyma drive drought resistance in neotropical trees. *Plant, Cell & Environment* **43**: 965–980.

**Jin Y, Qian H. 2019.** V.PHYLOMAKER: an R package that can generate very large phylogenies for vascular plants. *Ecography* **42**: 1353–1359.

**Kawai K, Minagi K, Nakamura T, Saiki S-T, Yazaki K, Ishida A. 2021.** Parenchyma underlies the interspecific variation of xylem hydraulics and carbon storage across 15 woody species on a subtropical Island in Japan. *Tree Physiology* **42**: 337–350.

**Kembel SW, Cowan PD, Helmus MR, Cornwell WK, Morlon H, Ackerly DD, Blomberg SP, Webb CO. 2010.** PICANTE: R tools for integrating phylogenies and ecology. *Bioinformatics* **26**: 1463–1464.

**Kiorapostolou N, Da Sois L, Petruzzellis F, Savi T, Trifilò P, Nardini A, Petit G. 2019.** Vulnerability to xylem embolism correlates to wood parenchyma fraction in angiosperms but not in gymnosperms. *Tree Physiology* **39**: 1675–1684.

**Kono Y, Ishida A, Saiki S-T, Yoshimura K, Dannoura M, Yazaki K, Kimura F, Yoshimura J, Aikawa S. 2019.** Initial hydraulic failure followed by late-stage carbon starvation leads to drought-induced death in the tree *Trema orientalis*. *Communications Biology* **2**: 1–9.

**Körner C. 2003.** Carbon limitation in trees. *Journal of Ecology* **91**: 4–17.

**Lachenbruch B, McCulloh KA. 2014.** Traits, properties, and performance: how woody plants combine hydraulic and mechanical functions in a cell, tissue, or whole plant. *New Phytologist* **204**: 747–764.

**Lens F, Sperry JS, Christman MA, Choat B, Rabaey D, Jansen S. 2011.** Testing hypotheses that link wood anatomy to cavitation resistance and hydraulic conductivity in the genus *Acer*. *New Phytologist* **190**: 709–723.

**Levionnois S, Salmon C, Alméras T, Clair B, Ziegler C, Coste S, Stahl C, González-Melo A, Heinz C, Heuret P. 2021.** Anatomies, vascular architectures, and mechanics underlying the leaf size-stem size spectrum in 42 Neotropical tree species. *Journal of Experimental Botany* **72**: 7957–7969.

**Lewis AM. 1992.** Measuring the hydraulic diameter of a pore or conduit. *American Journal of Botany* **79**: 1158–1161.

**Liu H, Gleason SM, Hao G, Hua L, He P, Goldstein G, Ye Q. 2019.** Hydraulic traits are coordinated with maximum plant height at the global scale. *Science Advances* **5**: eaav1332.

**Loepfe L, Martinez-Vilalta J, Piñol J, Mencuccini M. 2007.** The relevance of xylem network structure for plant hydraulic efficiency and safety. *Journal of Theoretical Biology* **247**: 788–803.

**Lübbe T, Lamarque LJ, Delzon S, Torres Ruiz JM, Burlett R, Leuschner C, Schuldt B. 2022.** High variation in hydraulic efficiency but not xylem safety between roots and branches in four temperate broad-leaved tree species. *Functional Ecology* **36**: 699–712.

**Maherali H, Moura CF, Caldeira MC, Willson CJ, Jackson RB. 2006.** Functional coordination between leaf gas exchange and vulnerability to xylem cavitation in temperate forest trees. *Plant, Cell & Environment* **29**: 571–583.

**Maherali H, Pockman WT, Jackson RB. 2004.** Adaptive variation in the vulnerability of woody plants to xylem cavitation. *Ecology* **85**: 2184–2199.

**Malaeb ZA, Summers JK, Pugesek BH. 2000.** Using structural equation modeling to investigate relationships among ecological variables. *Environmental and Ecological Statistics* **7**: 93–111.

**Markesteijn L, Poorter L, Bongers F, Paz H, Sack L. 2011.** Hydraulics and life history of tropical dry forest tree species: coordination of species' drought and shade tolerance. *New Phytologist* **191**: 480–495.

**Martínez-Cabrera HI, Jones CS, Espino S, Schenk HJ. 2009.** Wood anatomy and wood density in shrubs: responses to varying aridity along transcontinental transects. *American Journal of Botany* **96**: 1388–1398.

**Martínez-Vilalta J, Sala A, Asensio D, Galiano L, Hoch G, Palacio S, Piper FI, Lloret F. 2016.** Dynamics of non-structural carbohydrates in terrestrial plants: a global synthesis. *Ecological Monographs* **86**: 495–516.

**McCulloh K, Sperry JS, Lachenbruch B, Meinzer FC, Reich PB, Voelker S. 2010.** Moving water well: comparing hydraulic efficiency in twigs and trunks of coniferous, ring-porous, and diffuse-porous saplings from temperate and tropical forests. *New Phytologist* **186**: 439–450.

**McCulloh KA, Meinzer FC, Sperry JS, Lachenbruch B, Voelker SL, Woodruff DR, Domec J-C. 2011.** Comparative hydraulic architecture of tropical tree species representing a range of successional stages and wood density. *Oecologia* **167**: 27–37.

**Morris H, Gillingham MAF, Plavcová L, Gleason SM, Olson ME, Coomes DA, Fichtler E, Klepsch MM, Martínez-Cabrera HI, McGlinn DJ *et al.* 2018.** Vessel diameter is related to amount and spatial arrangement of axial parenchyma in woody angiosperms. *Plant, Cell & Environment* **41**: 245–260.

**Morris H, Hietala AM, Jansen S, Ribera J, Rosner S, Salmeia KA, Schwarze FW. 2020.** Using the CODIT model to explain secondary metabolites of xylem in defence systems of temperate trees against decay fungi. *Annals of Botany* **125**: 701–720.

**Morris H, Plavcová L, Cvecko P, Fichtler E, Gillingham MAF, Martínez-Cabrera HI, McGlinn DJ, Wheeler E, Zheng J, Ziemińska K *et al.* 2016.** A global analysis of parenchyma tissue fractions in secondary xylem of seed plants. *New Phytologist* **209**: 1553–1565.

**Naes T, Isaksson T, Fearn T, Davies T. 2004.** *A user-friendly guide to multivariate calibration and classification*. Chicester, UK: NIR Publications Press.

**Nardini A, Lo Gullo MA, Salleo S. 2011.** Refilling embolized xylem conduits: is it a matter of phloem unloading? *Plant Science* **180**: 604–611.

**Paradis E, Claude J, Strimmer K. 2004.** APE: analyses of phylogenetics and evolution in R language. *Bioinformatics* **20**: 289–290.

**Patel RN. 1965.** A comparison of the anatomy of the secondary xylem in roots and stems. *Holzforschung* **19**: 963–971.

**Pérez-Harguindeguy N, Díaz S, Garnier E, Lavorel S, Poorter H, Jaureguiberry P, Bret-Harte MS, Cornwell WK, Craine JM, Gurvich DE *et al.* 2016.** Corrigendum to: new handbook for standardised measurement of plant functional traits worldwide. *Australian Journal of Botany* **64**: 715–716.

**Peters JMR, Gauthey A, Lopez R, Carins-Murphy MR, Brodribb TJ, Choat B. 2020.** Non-invasive imaging reveals convergence in root and stem vulnerability to cavitation across five tree species. *Journal of Experimental Botany* **71**: 6623–6637.

**Plavcová L, Hoch G, Morris H, Ghiasi S, Jansen S. 2016.** The amount of parenchyma and living fibres affects storage of nonstructural carbohydrates in young stems and roots of temperate trees. *American Journal of Botany* **103**: 603–612.

**Poorter L, McDonald I, Alarcón A, Fichtler E, Licona J-C, Peña-Claros M, Sterck F, Villegas Z, Sass-Klaassen U. 2010.** The importance of wood traits and hydraulic conductance for the performance and life history strategies of 42 rainforest tree species. *New Phytologist* **185**: 481–492.

**Popp M, Lied W, Meyer AJ, Richter A, Schiller P, Schwitte H. 1996.** Sample preservation for determination of organic compounds: microwave versus freeze-drying. *Journal of Experimental Botany* **47**: 1469–1473.

**Pratt RB, Jacobsen AL. 2017.** Conflicting demands on angiosperm xylem: tradeoffs among storage, transport and biomechanics. *Plant, Cell & Environment* **40**: 897–913.

**Pratt RB, Jacobsen AL, Ewers FW, Davis SD. 2007.** Relationships among xylem transport, biomechanics and storage in stems and roots of nine Rhamnaceae species of the California chaparral. *New Phytologist* **174**: 787–798.

**Pratt RB, Jacobsen AL, Percolla MI, Guzman MED, Traugh CA, Tobin MF. 2021a.** Trade-offs among transport, support, and storage in xylem from shrubs in a semiarid chaparral environment tested with structural equation modeling. *Proceedings of the National Academy of Sciences, USA* **118**: e2104336118.

**Pratt RB, Tobin MF, Jacobsen AL, Traugh CA, Guzman MED, Hayes CC, Toschi HS, MacKinnon ED, Percolla MI, Clem ME *et al.* 2021b.** Starch storage capacity of sapwood is related to dehydration avoidance during drought. *American Journal of Botany* **108**: 91–101.

**R Development Core Team. 2020.** *R: a language and environment for statistical computing*. Vienna, Austria: R Foundation for Statistical Computing. [WWW document] URL https://www.R-project.org/ [accessed 06 May 2020].

**Ramirez JA, Posada JM, Handa IT, Hoch G, Vohland M, Messier C, Reu B. 2015.** Near-infrared spectroscopy (NIRS) predicts non-structural carbohydrate concentrations in different tissue types of a broad range of tree species. *Methods in Ecology and Evolution* **6**: 1018–1025.

**Rana R, Langenfeld-Heyser R, Finkeldey R, Polle A. 2009.** Functional anatomy of five endangered tropical timber wood species of the family Dipterocarpaceae. *Trees* **23**: 521–529.

**Rodríguez-Calcerrada J, López R, Salomón R, Gordaliza GG, Valbuena-Carabaña M, Oleksyn J, Gil L. 2015.** Stem $CO_2$ efflux in six co-occurring tree species: underlying factors and ecological implications. *Plant, Cell & Environment* **38**: 1104–1115.

**Rosado LR, Takarada LM, de Araújo ACC, de Souza KRD, Hein PRG, Rosado SC, Gonçalves FMA. 2019.** Near infrared spectroscopy: rapid and accurate analytical tool for prediction of non-structural carbohydrates in wood. *Cerne* **25**: 84–92.

**Rosseel Y. 2012.** LAVAAN: an R package for structural equation modeling. *Journal of Statistical Software* **48**: 1–36.

**Rowland L, da Costa ACL, Galbraith DR, Oliveira RS, Binks OJ, Oliveira AR, Pullen AM, Doughty CE, Metcalfe DB, Vasconcelos SS *et al.* 2015.** Death from drought in tropical forests is triggered by hydraulics not carbon starvation. *Nature* **528**: 119–122.

**Sala A, Woodruff DR, Meinzer FC. 2012.** Carbon dynamics in trees: feast or famine? *Tree Physiology* **32**: 764–775.

**Savitzky A, Golay MJE. 1964.** Smoothing and differentiation of data by simplified least squares procedures. *Analytical Chemistry* **36**: 1627–1639.

**Schuldt B, Leuschner C, Brock N, Horna V. 2013.** Changes in wood density, wood anatomy and hydraulic properties of the xylem along the root-to-shoot flow path in tropical rainforest trees. *Tree Physiology* **33**: 161–174.

**Secchi F, Pagliarani C, Zwieniecki MA. 2017.** The functional role of xylem parenchyma cells and aquaporins during recovery from severe water stress. *Plant, Cell & Environment* **40**: 858–871.

**Smith MG, Miller RE, Arndt SK, Kasel S, Bennett LT. 2018.** Whole-tree distribution and temporal variation of non-structural carbohydrates in broadleaf evergreen trees. *Tree Physiology* **38**: 570–581.

**Smith SA, Brown JW. 2018.** Constructing a broadly inclusive seed plant phylogeny. *American Journal of Botany* **105**: 302–314.

**Smith VC, Ennos AR. 2003.** The effects of air flow and stem flexure on the mechanical and hydraulic properties of the stems of sunflowers *Helianthus annuus* L. *Journal of Experimental Botany* **54**: 845–849.

**Sperry JS, Hacke UG, Wheeler JK. 2005.** Comparative analysis of end wall resistivity in xylem conduits. *Plant, Cell & Environment* **28**: 456–465.

**Sperry JS, Ikeda T. 1997.** Xylem cavitation in roots and stems of Douglas-fir and white fir. *Tree Physiology* **17**: 275–280.

**Sperry JS, Sullivan JEM. 1992.** Xylem embolism in response to freeze-thaw cycles and water stress in ring-porous, diffuse-porous, and conifer species. *Plant Physiology* **100**: 605–613.

**Stokes A, Guitard D. 1997.** Tree root response to mechanical stress. In: Altman A, Waisel Y, eds. *Biology of root formation and development*. Boston, MA, USA: Springer, 227–236.

**Tomasella M, Petrussa E, Petruzzellis F, Nardini A, Casolo V. 2020.** The possible role of non-structural carbohydrates in the regulation of tree hydraulics. *International Journal of Molecular Sciences* **21**: 144.

**Tyree MT, Ewers FW. 1991.** The hydraulic architecture of trees and other woody plants. *New Phytologist* **119**: 345–360.

**Van Handel E. 1965.** Estimation of glycogen in small amounts of tissue. *Analytical Biochemistry* **11**: 256–265.

**Wang L, Dai Y, Zhang J, Meng P, Wan X. 2022.** Xylem structure and hydraulic characteristics of deep roots, shallow roots and branches of walnut under seasonal drought. *BMC Plant Biology* **22**: 440.

**Warton DI, Duursma RA, Falster DS, Taskinen S. 2012.** SMATR 3 – an R package for estimation and inference about allometric lines. *Methods in Ecology and Evolution* **3**: 257–259.

**Warton DI, Wright IJ, Falster DS, Westoby M. 2006.** Bivariate line-fitting methods for allometry. *Biological Reviews* **81**: 259–291.

**Wegner LH. 2014.** Root pressure and beyond: energetically uphill water transport into xylem vessels? *Journal of Experimental Botany* **65**: 381–393.

**Wheeler EA, Baas P, Gasson PE. 1989.** IAWA list of microscopic features for hardwood identification. *The IAWA Journal* **10**: 219–332.

**Wiemann MC, Williamson GB. 2002.** Geographic variation in wood specific gravity: effects of latitude, temperature, and precipitation. *Wood and Fibre Science* **34**: 96–107.

**Williamson GB, Wiemann MC. 2010.** Measuring wood specific gravity. . . correctly. *American Journal of Botany* **97**: 519–524.

**Woodrum CL, Ewers FW, Telewski FW. 2003.** Hydraulic, biomechanical, and anatomical interactions of xylem from five species of *Acer* (Aceraceae). *American Journal of Botany* **90**: 693–699.

**Wu M, Zhang Y, Oya T, Marcati CR, Pereira L, Jansen S. 2020.** Root xylem in three woody angiosperm species is not more vulnerable to embolism than stem xylem. *Plant and Soil* **450**: 479–495.

**Yamada Y, Awano T, Fujita M, Takabe K. 2011.** Living wood fibers act as large-capacity "single-use" starch storage in black locust (*Robinia pseudoacacia*). *Trees* **25**: 607–616.

**Yoshimura K, Saiki S-T, Yazaki K, Ogasa MY, Shirai M, Nakano T, Yoshimura J, Ishida A. 2016.** The dynamics of carbon stored in xylem sapwood to drought-induced hydraulic stress in mature trees. *Scientific Reports* **6**: 24513.

**Zanne AE, Westoby M, Falster DS, Ackerly DD, Loarie SR, Arnold SEJ, Coomes DA. 2010.** Angiosperm wood structure: global patterns in vessel anatomy and their relation to wood density and potential conductivity. *American Journal of Botany* **97**: 207–215.

**Zhang G, Maillard P, Mao Z, Brancheriau L, Engel J, Gerard B, Fortunel C, Maeght JL, Martínez-Vilalta J, Ramel M *et al.* 2022a.** Non-structural carbohydrates and morphological traits of leaves, stems and roots from tree species in different climates. *BMC Research Notes* **15**: 251.

**Zhang G, Mao Z, Fortunel C, Martínez-Vilalta J, Viennois G, Maillard P, Stokes A. 2022b.** Parenchyma fractions drive the storage capacity of non-structural carbohydrates across a broad range of tree species. *American Journal of Botany* **109**: 535–549.

**Zheng J, Martínez-Cabrera HI. 2013.** Wood anatomical correlates with theoretical conductivity and wood density across China: evolutionary evidence of the functional differentiation of axial and radial parenchyma. *Annals of Botany* **112**: 927–935.

**Zheng J, Zhao X, Morris H, Jansen S. 2019.** Phylogeny best explains latitudinal patterns of xylem tissue fractions for woody angiosperm species across China. *Frontiers in Plant Science* **10**: 556.

**Zheng P, Aoki D, Matsushita Y, Yagami S, Sano Y, Yoshida M, Fukushima K. 2016.** Lignification of ray parenchyma cells (RPCs) in the xylem of *Phellodendron amurense* Rupr.: quantitative and structural investigation by TOF-SIMS and thioacidolysis of laser microdissection cuts of RPCs. *Holzforschung* **70**: 641–652.

**Ziegler C, Coste S, Stahl C, Delzon S, Levionnois S, Cazal J, Cochard H, Esquivel-Muelbert A, Goret J-Y, Heuret P *et al.* 2019.** Large hydraulic safety margins protect Neotropical canopy rainforest tree species against hydraulic failure during drought. *Annals of Forest Science* **76**: 1–18.

**Ziemińska K, Butler DW, Gleason SM, Wright IJ, Westoby M. 2013.** Fibre wall and lumen fractions drive wood density variation across 24 Australian angiosperms. *AoB Plants* **5**: plt046.

**Ziemińska K, Rosa E, Gleason SM, Holbrook NM. 2020.** Wood day capacitance is related to water content, wood density, and anatomy across 30 temperate tree species. *Plant, Cell & Environment* **43**: 3048–3067.

## Supporting Information

Additional Supporting Information may be found online in the Supporting Information section at the end of the article.

**Fig. S1** Mean monthly climatic data for temperate, Mediterranean and tropical sites (data are means from 1990 to 2020).

**Fig. S2** Light microscopy images of transverse sections of *Micropholis guyanensis*.

**Fig. S3** Phylogenetic tree of the 60 tree species.

**Fig. S4** Stack bar graph of stem cellular fractions across 60 species.

**Fig. S5** Stack bar graph of root cellular fractions across 60 species.

**Fig. S6** Boxplot of radial parenchyma, axial parenchyma, vessel mean diameter, vessel density, soluble sugars and starch in stem and root xylem across from temperate, Mediterranean and tropical climates.

**Fig. S7** Structural equation model for displaying trade-offs among cellular fractions and the functions commonly associated with these traits in stem and root from 60 species in temperate, Mediterranean and tropical climates.

**Table S1** Summary of previous studies on trade-offs between xylem structure and function.

**Table S2** Tree species list with diameter at breast height, GPS coordinates, type of vessel porosity and tracheid occurrence.

**Table S3** Model parameters of near-infrared spectroscopy calibration for contents of soluble sugars and starch.

**Table S4** Standardized major axis regressions model parameters for stem wood traits pairs among temperate, Mediterranean and tropical climates.

**Table S5** Standardized major axis regressions model parameters for root wood traits pairs among temperate, Mediterranean and tropical climates.

**Table S6** Comparison of pairwise wood trait correlation matrices between Pearson's test with and without phylogenetically independent contrasts.

**Table S7** Blomberg's *K* values for wood traits of stem and root across 60 species.

Please note: Wiley is not responsible for the content or functionality of any Supporting Information supplied by the authors. Any queries (other than missing material) should be directed to the *New Phytologist* Central Office.